Electrical Fast-Transient Tests: Applications and Limitations

FRANÇOIS D. MARTZLOFF, FELLOW, IEEE, AND THOMAS F. LEEDY, MEMBER, IEEE

Abstract—**According to a new standard of the International Electrotechnical Commission (IEC), a fast-transient test must be applied to the connecting cables of electronic equipment. The purpose of the test is to demonstrate equipment immunity to fast transients resulting from switching. Tests and simulations of the propagation and attenuation of these fast transients in typical connecting cables are described, placing the IEC requirements in perspective.**

Introduction

CONTINUING technical progress in the performance of electronic control systems has been made possible by fast logic devices operating at low levels of voltage and power, with high component density and interactive peripherals. These undisputed advantages, however, can make the circuits increasingly sensitive to external interfering overvoltages resulting in amplitude-related hardware failures or rate-of-change-related system upsets. To guard against such effects, immunity to such failure must be demonstrated by realistic tests which validate the design rules and installation practices of the equipment. However, a balance must be found between overdesign and cost limitations.

In contrast with traditional surge testing aimed at validating insulation levels or the energy-handling capability of surge protection devices, recent proposals advocate fast-transient tests demonstrating interference immunity. The new test waveforms represent electrostatic discharge effects or reignitions occurring during switching sequences. The basis for such proposals is an increasing awareness of the significance of fast transients. This new awareness results from two factors: 1) increases in the bandwidth and writing speed of oscilloscopes which makes possible the detailed observation and measurement of these phenomena, and 2) field failures of equipment which pass traditional tests but fail when subjected to the new fast-transient tests.

The rationale for requiring the new tests is based on the assumption that interfering transients generated by power circuit switching will couple into adjacent power or signal lines. These interfering transients will then propagate toward susceptible equipment. The fast transients contain high-frequency components that are expected intuitively to suffer greater attenuation than low-frequency components as they propagate in the lines. Verifying and quantifying this intuitive expectation provides a perspective on the severity of the situation and helps define realistic test requirements. To that end, this paper describes specific measurements conducted for typical low-voltage power line configurations. An attenuation model is proposed which provides a tool for understanding the significance of the line parameters and extends the usefulness of the results to general cases.

Paper PID 89-09, approved by the Petroleum and Chemical Industry Committee of the IEEE Industry Applications Society for presentation at the 1989 Petroleum and Chemical Industry Committee Technical Conference, San Diego, CA, September 11-13, and at the 1989 IEEE Industry Applications Society Annual Meeting, San Diego, CA, October 1-5. Manuscript released for publication February 22, 1989.

The authors are with the Electricity Division, National Institute of Standards and Technology, Building 220, Room B-344, U.S. Department of Commerce, Gaithersburg, MD 20899.

IEEE Log Number 8931459.

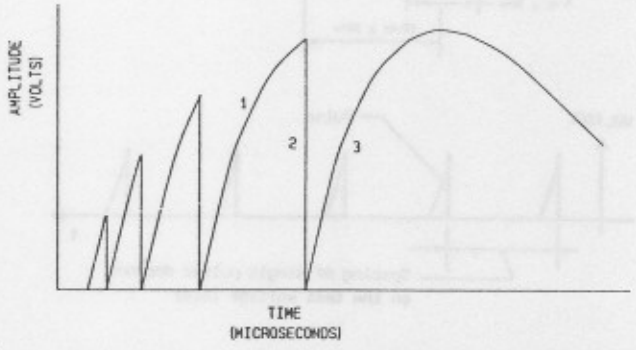

Fig. 1. Typical transient produced by contact opening. 1: voltage recovery of circuit (kHz frequency); 2: reignition (ns collapse); 3: complete recovery (μs duration).

The IEC Electrical Fast Transient Test

The Technical Committee TC65 of the International Electrotechnical Commission (IEC) has completed a document [1] requiring immunity of industrial process control equipment to fast transients be demonstrated. According to that document, fast transients must be applied to the incoming power lines as well as to the input/output data lines of this equipment.

The origin of fast transients is the well-known behavior of some air contactors when they interrupt an inductive–capacitive circuit: as the contacts part, the arc drawn between the contacts becomes unstable and the current is then interrupted, only to be re-established promptly by reignition across the gap. A race occurs between the dielectric strength of the increasing gap, and the voltage recovery of the circuit. Consequently, a sequence of clearing and reignition ensues, with an eventual full clearing of the circuit. As shown in Fig. 1, each of the clearings produces the beginning of an oscillation at relatively low frequency depending on the local circuit parameters. As the voltage across the gap increases at a rate corresponding to this frequency, reignition occurs if the gap withstand voltage is exceeded. The waveform of each

0093-9994/90/0100-0151$01.00

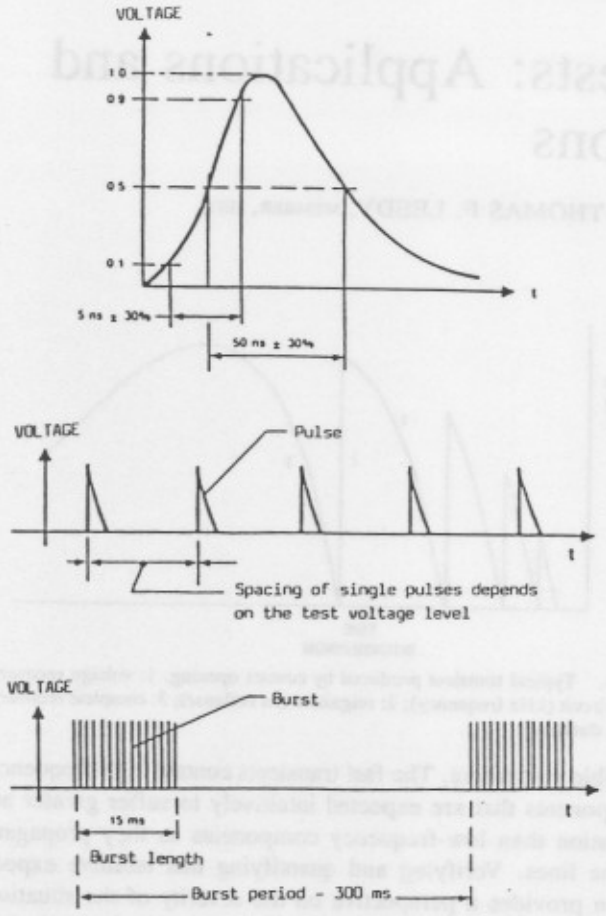

Fig. 2. Fast-transients specified by IEC 801-4. Top: waveshape of single pulse for 50-Ω load.

sequence is then a series of pulses, each with a relatively slow voltage rise followed by collapse in a few nanoseconds.

Thus the circuit behaves as a generator of transient pulse bursts. Each pulse has a slow rise ending in an abrupt collapse. Because the pulses occur in bursts, these single pulses have the same effect as pulses with fast rise time and slower decay. For standardization purposes, the IEC document specifies an electrical fast transient (EFT) 5/50-ns waveform as shown in Fig. 2, where the rise time is 5 ns and the duration (full width at half maximum) is 50 ns. The repetition rate of the pulses within a burst is not specified. However, the duration of the burst and the interval between bursts are specified.

Three limitations exist in the severity of the situation, resulting from the fast transient nature of the test and the conditions of application.

1) As described in the IEC test procedure, the test transients are coupled to the equipment under test (EUT) by a capacitive "clamp" through which the power or data cable is inserted. This clamp is a mechanical test fixture consisting of two hinged metallic plates designed to provide a fixed and repeatable capacitance between the output of the pulse generator and the input cables. Discrete capacitors can also provide the coupling. This coupling method produces a capacitive divider: the high side of the divider is the coupling capacitor, and the low side is the internal capacitance to ground of the EUT (Fig. 3). This effect, therefore, is influenced by the design of the

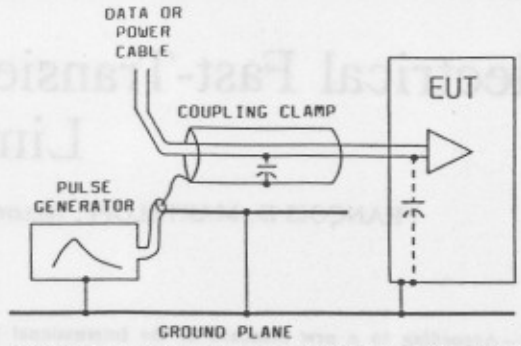

Fig. 3. Coupling electrical fast transient (EFT) pulses into equipment cables.

equipment and becomes a design parameter controlled by each manufacturer.

2) The freedom left to those who perform the test on setting the repetition rate of the pulses leaves some ambiguity on the total number of the pulses applied to the EUT. The test presumably aims at identifying an interference with the logic of the circuit. That interference is likely to occur during critical state transitions of the semiconductor circuitry of the equipment, making timing and coincidence very significant. Advocates of electrostatic discharge tests make a case that up to 10 000 pulses should be applied at random to produce a high degree of confidence that the issue of pulse timing has been addressed [2].

3) In an actual installation, attenuation between the point of coupling and the victim equipment will reduce the severity of the impinging transient. The line propagation characteristics reduce the peak amplitude and increase the rise time of the pulse as it travels down the line. This effect, therefore, is influenced by the line regardless of this equipment design. Although our measurements and modeling address this third limitation, the two other limitations should also be kept in mind.

Line Configurations

Two line configurations were selected as typical of low-voltage power lines: a three-conductor line in a steel conduit, and a three-conductor cable with a nonmetallic jacket. The steel conduit line is easy to set up in the laboratory by arranging conduit sections in a zig-zag pattern. This arrangement allows placing the start and the end of the line next to each other to minimize the distance between the oscilloscope used for measuring the signals at either end of the line. At one end of the line, called the "sending end," single pulses with the IEC EFT waveform were injected. At the other end, called the "receiving end," the arriving pulses were recorded for various line terminating impedance configurations. The same oscilloscope was used to measure the waveforms at the two ends of the line. Thus the voltage ratios of the waveforms do not depend on the absolute accuracy of the instrumentation. In addition, the differential connection of the oscilloscope probes allows measurement without introducing an additional ground in the line, which is already grounded by its connection to the pulse generator. This arrangement also removes any question of variations of the stray capacitances to ground, provided that

the instruments stay in the same position for the two measurements, at both the sending and receiving end. The experimental details of the measurements are discussed in Appendix I.

Because the conduit contains the electromagnetic fields associated with the propagating pulse, there is no need to be concerned with coupling between adjacent sections of the line in the zig-zag, nor with losses by radiation from the line acting as an antenna. For the nonmetallic jacketed line, however, these effects must be addressed.

To investigate the effect of radiation losses from the nonmetallic jacketed line, three experiments were performed outdoors. First, measurements were made with the line arranged in a wide loop, elevated from ground and away from metallic objects. To assess the importance of the proximity of the line to ground, the line was later dropped to ground level and a second set of measurements was made. Last, a coil of identical cable was also subjected to the same measurements. The observed difference of the three sets of measurements was negligible for practical purposes.

For the case of the conduit-enclosed line, a previous paper reports in detail the experimental results and theoretical expectations from a model solely based on the geometry of the line [3]. As a convenience for the readers and for comparison with the new results on nonmetallic jacket line, the results of the first configuration are summarized here. For the nonmetallic line, we used a new model based on measurable electrical parameters of the line, rather than the geometry of the line. Appendix I gives details on instrumentation considerations; Appendix II gives details on the line propagation model.

Steel Conduit Line

A representative low-voltage indoor single-phase power line was installed in the laboratory, with three conductors in a steel conduit. The line length was 63 m (20 thin-wall conduit sections, each the standard 10-ft length), using typical industrial components such as wire nuts at the splices in the wire. Three insulated (600 V) copper conductors of number 14 AWG (1.6 mm diameter), pulled in the 20-mm diameter conduit (1/2 EMT), represent the phase, neutral, and grounding conductors. At the sending end, the neutral conductor was bonded to the grounding conductor and to the conduit.

At the receiving end, the neutral conductor was not bonded to the grounding conductor, nor to the conduit. This type of connection is typical U.S. practice for a branch circuit originating at a service entrance.

For modeling purposes, it is much easier to assume that the line is uniform. In practice, the location of the conductors vary within the conduit due to sag, bends, or crossed wires. Therefore, we considered two limiting cases: 1) the wires are located at the center of the conduit, separated from each other by the thickness of the wire insulation, and 2) the wires are located against the wall of the conduit. In the numerical analysis, a model parameter k accounted for these two positions. A detailed description of the analysis is given in [3].

Fig. 4 shows the composite results of the measurements and modeling for the IEC EFT pulse arriving at the receiving end. The results are expressed as a percentage of the pulse applied

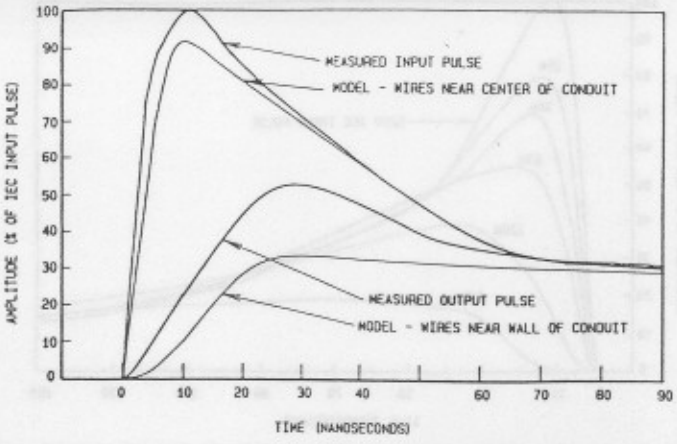

Fig. 4. Composite plot of measured and modeled pulses, as percent of amplitude, for wires enclosed in metal conduit.

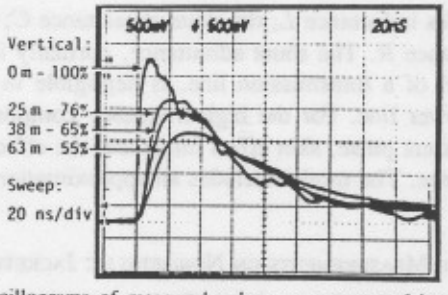

Fig. 5. Oscillograms of measured pulses, as percent of input amplitude (0 m), for various lengths of wires enclosed in metal conduit (25, 38, and 63 m).

at the sending end. All the measurements were made with a injected pulse of 2.5 or 5 V, to avoid the problems of electromagnetic interference or safety associated with the levels of 500–4000 V specified by the IEC standard. The linearity of the circuits allows this simplification. The pulse, measured at the receiving end, is 50 percent of the sending-end pulse and lies between the two limiting cases of the model. Qualitatively, the model pulses look very much like the measured pulses. From the position of the measured pulse with respect to the two limiting cases, we can then assign a value to the model parameter k such that attenuation for the 63-m line is accurately matched. Given this empirically determined value, the model will show the effect of varying the line length.

Measurements for several line lengths (Fig. 5) show receiving-end peak amplitudes of 76 and 65 percent of the sending-end peak amplitude for 25- and 38-m lines, respectively. Corresponding peak amplitudes predicted by the model are 75 and 67 percent (Fig. 6). For the greater line lengths, where measurements would be cumbersome, the model can now readily provide the answers. Fig. 6 includes examples for 120- and 240-m lengths, showing the continued attenuation and smearing of the pulse as the line length increases.

Nonmetallic Jacketed Line

For this type of line, the insulation holds the conductors in a fixed and uniform geometry relative to each other, in contrast with the random location of the conductors pulled in a conduit. It is possible to determine, by a simple set of measurements or calculations, the parameters of the transmission

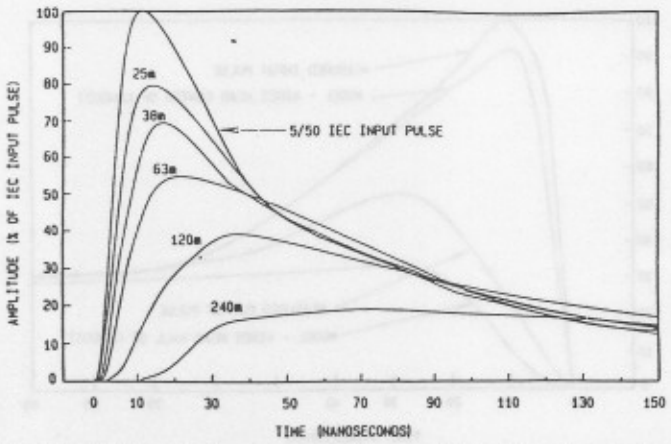

Fig. 6. Model prediction, as percent of input amplitude, for various lengths of wires enclosed in metal conduit.

line: the series inductance L; the shunt capacitance C; and the series resistance R. The shunt admittance, normally included in the model of a transmission line, is negligible in a well-insulated power line. For the high-frequency components of the fast-transient pulse, skin effect influences the effective series impedance. The model includes an approximation of this effect.

Experimental Measurements on Nonmetallic Jacketed Lines

The 75-m line (250 ft) consisted of a neoprene-jacketed cord with three number 14 AWG (1.6-mm diameter) neoprene-insulated copper conductors. The line was suspended 2 m above ground. The line was arranged in a triangular loop with the sending end and the receiving end at one corner of the triangle. In this manner, either end could be connected to the oscilloscope. As described in Appendix I, a constant impedance load was maintained at the sending end by using a dummy load when switching the oscilloscope from the sending end to the receiving end. In all the measurements, two of the conductors were bonded at the sending end, representing the neutral and the grounding conductors. At the receiving end, the arriving pulse was recorded for various terminating load combinations. Fig. 7 shows an EFT signal with 2.5 V peak and 5/50-ns waveform injected at the sending end, arriving as a 30/110-ns signal at the end of the line. This peak amplitude of 48 percent is very close to the 50-percent value found for the steel conduit. The small difference between the two values is due to the oscillogram reading uncertainty rather than to a significant difference between the characteristics of the two lines. The question raised in the introduction, concerning radiation losses, is answered in the negative—or at least in the form, "not discernable at this level of significance."

Need to Consider Loading at Receiving End

Classical transmission line theory points out that reflections occur at the receiving end of the line when the terminating impedance differs from the characteristic impedance of the cable: 1) doubling the arriving pulse for an open end (and thus reflecting a pulse of the same polarity); 2) maintaining zero for a shorted end (and thus reflecting a pulse of reverse polarity); and 3) maintaining the level unchanged for a terminating

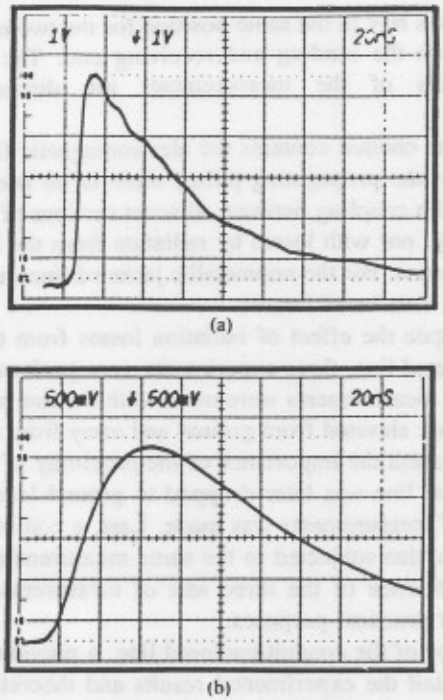

Fig. 7. Pulses for nonmetallic jacketed cable. (a) Sending-end pulse. Vertical: 1 V/div, sweep: 20 ns/div. Signal parameters: amplitude = 5 V (100 percent), rise time = 5 ns, FWHM = 50 ns. (b) Receiving-end pulse. Vertical: 0.5 V/div, sweep: 20 ns/div. Signal parameters: amplitude = 2.4 V (48 percent), rise time: 30 ns, FWHM: 110 ns.

impedance that matches the line characteristic impedance (and thus having no reflection).

Measurements made with "slow" 1.2/50-μs impulses have shown that, while correct, this analysis does not produce useful results if applied to line lengths that do not contain the whole impulse front [4]. For a 1.2-μs front in a line where the propagation velocity is approximately 2/3 the speed of light in vacuum (300 m/μs), this lower limit on line length is approximately 200 m. For the 5/50-ns IEC EFT pulse, the 63-m line produces at the receiving end a 30-ns front time. According to the model, a 240-m line would produce a 60-ns front time (Fig. 6). Clearly, then, for this short an impulse, the receiving-end terminating impedance effects must be considered according to classical transmission line theory.

Because the measurement system has an impedance of 100 Ω while the characteristic impedances of the lines investigated are approximately 60 Ω, the case of an open-ended line cannot be measured. In actual installations and in the absence of a low-impedance instrument, the pulse would have twice the amplitude shown in Fig. 7. An open end is the limiting case for a very light load such as a control circuit during the off cycle of the power circuit. Adding even a small admittance at the end of the line substantially reduces the doubling effect.

Common-Mode and Normal-Mode Coupling

The method specified by IEC 801-4 for coupling the test transients to the power or the data cables introduces them as a common-mode signal in the cable (Fig. 3). This situation is not explicitly pointed out in the IEC document, but it must be clearly understood. Another standard advocating fast transients [5] specifies the application of the test transients in any

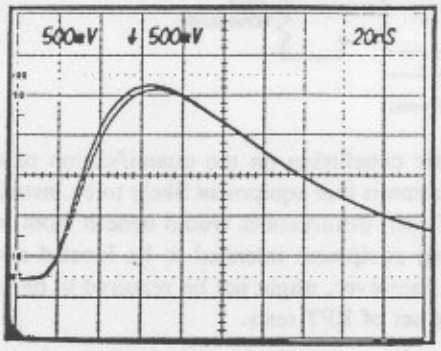

Fig. 8. Superimposed oscillograms of pulses at receiving-end, showing small difference between overhead line (left) and coiled line (right).

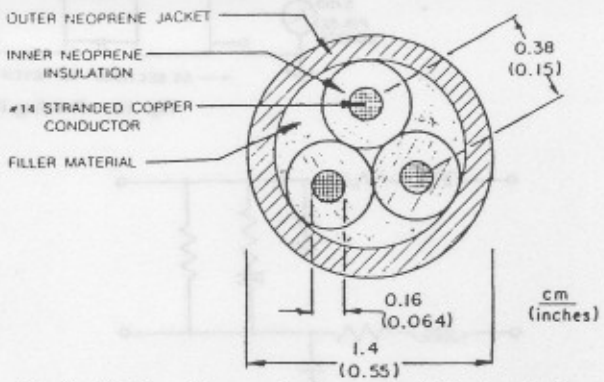

Fig. 9. Section of three-conductor, nonmetallic jacketed cable.

possible combination of the conductors for all input and output ports. While space and scope limitations for this paper prevent a comprehensive discussion of the subject, alerting readers to the issue is worthwhile.

The IEC EFT test focuses on installed equipment rather than on stand-alone equipment. The coupling clamp method for injecting the transients into the circuits is a very convenient procedure when cables are accessible. Practitioners of this test also report useful results by coupling the transients with foil wrapped around installed bundles of cables. The document provides detailed descriptions of the configuration for a laboratory test in an effort to ensure reproducible results. However, propagation, coupling, and attenuation effects associated with the capacitive divider nature of the test application will be strongly affected by small changes in the test circuit geometry, making the test difficult to describe and reproduce in absolute terms.

These remarks should not be construed as a criticism of the test. Anecdotal field experience shows that equipment with demonstrated immunity to the IEC 801-4 EFT procedure is less likely to be disturbed than equipment not meeting this requirement. The addition of the new test procedure has contributed to improved reliability. Experience is the ultimate validation of the usefulness of any performance standard.

No Practical Need for Outdoor Tests

After completing the tests on the suspended aboveground line, the line was lowered to ground (dry grass) level, and one set of measurements was made under that condition. The same measurements were also made on a control coil of identical cable, left in its original packing carton. These two control measurements show detectable but insignificant differences (Fig. 8) in the pulse arriving at the receiving end. Thus concern over line geometry and coiled versus "free space" configurations, while technically correct, is a negligible factor in practical applications. Therefore, future experimenters need not go outdoors to perform measurements, even at the higher frequencies since the coiled versus free space configurations appear to produce similar results. This finding extends the conclusion previously reached for 100-kHz ring waves [6].

Modeling the Propagation

Line Model

An electrical circuit analysis model was devised to investigate the changes in the voltage amplitude and waveform shape of the 5/50-ns EFT pulse as it propagates along a length of typical low-voltage power line. The low-voltage cable consists of three number 14 (1.6-mm diameter) conductors, with individual neoprene insulation and covered with a neoprene jacket. Fig. 9 shows a cross section of this cable.

A 63-m length of cable was simulated as 63 1-m lengths connected in series (Fig. 10). Each 1-m length was represented by the equivalent twoport subcircuit shown in Fig. 11. The subcircuit values represent the series and parallel elements of the two-conductor line, to which a capacitance from each wire to a hypothetical ground plane was added. Numerical values were assigned to these parameters as described in Appendix II.

Electrical circuit analysis simulations were performed using the SABER software system[1] which allows the 1-m subcircuit of Fig. 11 to be described only once as a "template." The software template is then replicated as many times as necessary to represent the transmission line. To investigate the effects of a change of a modeling parameter, such as a resistance or capacitance, the parameter need be changed only once in the data set. The 5/50-ns IEC EFT pulse was digitized from an oscillogram recorded during the experimental measurements so that a piecewise linear voltage source could be constructed for the circuit simulation.

Modeling Results

Fig. 12 shows the comparison of the observed (solid line) and the simulated (dashed line) waveforms at the end of 63 m of cable in response to the 5/50-ns IEC EFT pulse. The pulse simulated by the simple model described demonstrates the same general waveshape, rate of voltage rise, and amplitude as the observed pulse. The simulated pulse, however, has a shorter time duration than the observed pulse. In addition, the propagation velocity of the pulse, as predicted by the model, is slightly greater than the propagation velocity measured in the cable.

The discrepancies between the simulated and the observed waveforms and the velocities may be explained by several limitations of the model. First, the model did not consider the skin effect of the conductors. The skin effect would raise the resistance and inductance of the conductors for the high-frequency components of the waveform. Secondly, the cable consisted of

[1]SABER is a product of Analogy, Inc., Beaverton, OR.

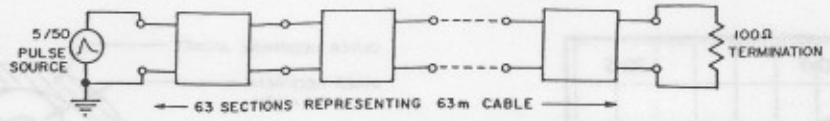

Fig. 10. Building line with repeated sections.

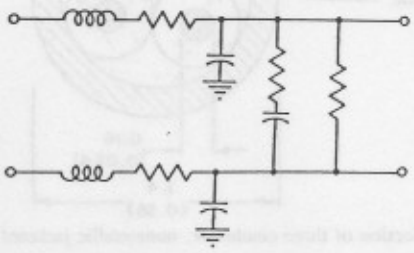

Fig. 11. Circuit parameters for individual sections.

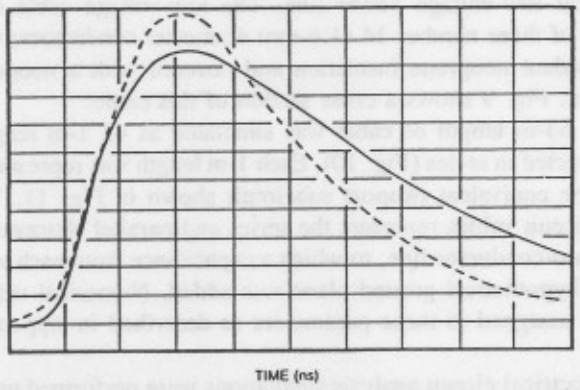

Fig. 12. Comparison between measured and modeled pulses at receiving end of nonmetallic jacketed line. Solid line: measured data; dashed line: predicted data.

three conductors of which only two were modeled. The third conductor was connected to ground at the pulse generator end of the cable and left open at the receiving end of the cable. The presence of this third conductor would change the propagation characteristics of the cable slightly. Finally, a simple loss model (a series *RC* network) has been assumed for the capacitance associated with the neoprene dielectric of the cable. The response at high frequencies of organic dielectrics may be considerably more complicated than this model reflects.

Conclusion

The two line configurations and their models yield similar results for measurements and for computations. Some difference might be expected between the quasi-coaxial configuration of a conduit-enclosed line and the open-line configuration with unshielded conductors of a nonmetallic jacket.

The effects of propagation of an EFT pulse in the lines are a reduction in the amplitude, a decrease in the steepness of the front, and an increase in the duration of the pulse. The first two effects reduce the severity of a pulse arriving at the victim equipment; the third effect is less significant for victim equipment sensitive to rate-of-change disturbances.

The two models provide the tools for analysis of other configurations. The choice of the geometry model or the electrical parameter model will depend on the available software and preferences of the investigator.

A pragmatic conclusion on the quantification of the EFT pulse propagation is that equipment likely to be installed close to sources of such disturbances would benefit from immunity demonstration; equipment intended to be located away from such sources, however, might not be required to be subjected to a complete set of EFT tests.

Acknowledgment

P. F. Wilson (former staff member of the National Bureau of Standards, Boulder, CO) developed the model [3] for the conduit line, which is only summarized here. The nonmetallic jacket measurements were funded in part by a consortium of private sector companies coordinated by Building Industry Consulting Service International of Tampa, FL.

Appendix I

Instrumentation

The voltages were recorded with a 1-GHz bandwidth oscilloscope and two 50-Ω input vertical preamplifiers. The mainframe of the oscilloscope performed the differential combination of the two signals. In this configuration, the bandwidth of the system is only 500 MHz, compared to the 1-GHz capability of the single-ended measurements with one preamplifier. This reduction in performance is an acceptable trade-off to obtain the differential connection of the probes. In the experiments, the conduit, oscilloscope chassis, and low-side output of the generator are bonded together and hence ensure minimum noise coupling. Where high voltages are involved, this configuration also provides improved safety. This was not a concern here as the measurement on this linear system were conducted with signals in the 5-V range. A check on the common mode rejection of the system indicated less than five-percent residual signal, an insignificant effect compared to the attenuation levels measured.

The preamplifiers have a 50-Ω input impedance, so that the effective impedance of the differentially connected probe is 100 Ω. At the sending end, the voltages of the line and neutral conductors with respect to chassis ground were each fed to one of the preamplifiers (Fig. 13). Thus the pulse delivered by the generator impinges on an impedance consisting of the two amplifiers in series, in parallel with the line. To make measurements at the receiving end, the same oscilloscope was used with its differential probes. However, the pulse arriving at the receiving end would experience a reflection due to any impedance mismatch. To obtain an impedance match, time-domain reflectometry was used to trim the terminating load until a minimal reflection occurred.

Good matching occurred with a 75-Ω termination for the steel conduit line (300-Ω trim in parallel with the 100-Ω probes). For the nonmetallic-jacketed cable, a 50-Ω termination gave best result (100-Ω trim and 100-Ω probes in parallel). For the steel conduit line, a dummy load was used, made

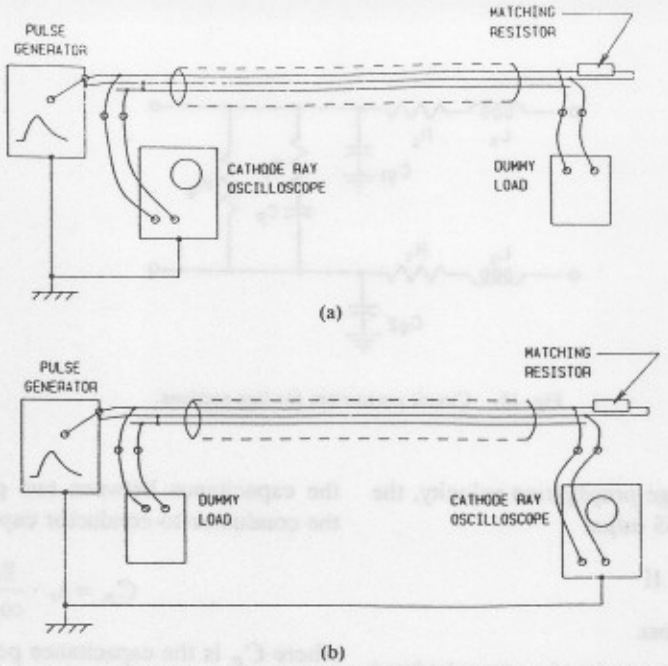

Fig. 13. Configuration for constant-load measurements with dummy load and single oscilloscope. (a) Measurement at sending end. (b) Measurement at receiving end.

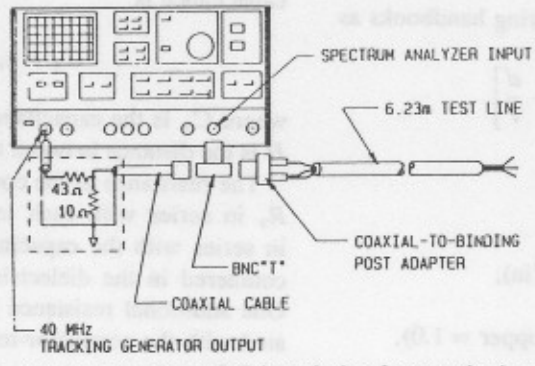

Fig. 14. Configuration for determining velocity of propagation in nonmetallic jacketed line.

of two 50-Ω coaxial terminators to provide the same matching impedance as that of the oscilloscope probes, as shown in Fig. 13. For the nonmetallic-jacketed cable measurements, two preamplifiers of the same type as the measuring preamplifiers, in a compatible mainframe, were used as the dummy load. In this manner, when recording the receiving-end waveforms with the measurement oscilloscope, the dummy load connected in parallel with the line at the sending end maintained a constant impedance load on the pulse generator.

The propagation velocity in the cable was measured as reported previously: a 40-MHz spectrum analyzer, with a tracking generator output, was used to determine the frequencies at which the input impedance of a length of cable is minimum [6]. Fig. 14 shows schematically the test line, the spectrum analyzer, and a resistive attenuator to improve the decoupling of the tracking generator output from the test line.

Fig. 15 shows the spectrum for a 6.23-m length of open-circuited test line. Voltage minima occur at 5.64, 19.4, and 30.4 MHz, corresponding to wavelengths of $\lambda/4$, $3\lambda/4$,

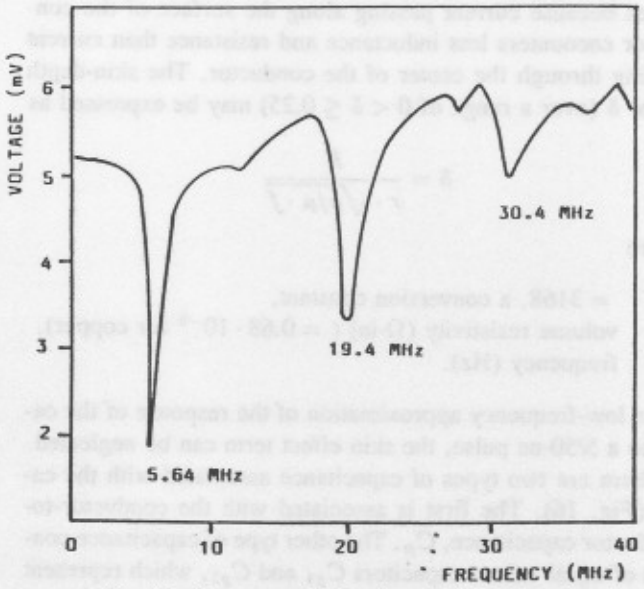

Fig. 15. Spectrum of 6.23-m length of test line.

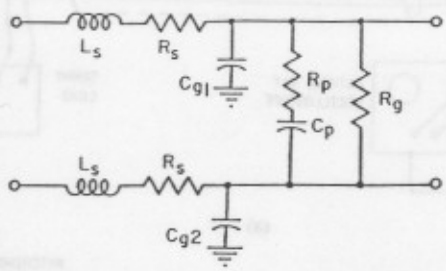

Fig. 16. Circuit parameters for line sections.

and 5λ/4, respectively. The average propagation velocity, the product of λ and frequency, is 155 m/μs.

Appendix II

Line Model

The series inductance of the 1-m section L_s was calculated using the formula for the inductance of two parallel conductors in close proximity to each other, with current in opposite directions in each conductor [7]. For such a situation, the effective inductance L_e is given in engineering handbooks as

$$L_e = 5 \cdot l \left[\ln \frac{d}{r} + \mu \cdot \delta - \frac{d}{l} \right]$$

where

- L_e effective inductance (nH),
- l length of the cable (in),
- d distance between the conductors (in),
- r radius of the conductors (in),
- μ relative magnetic permeability (copper = 1.0),
- δ skin depth factor.

The skin effect is a phenomenon affecting the conduction of cables because current passing along the surface of the conductor encounters less inductance and resistance than current passing through the center of the conductor. The skin-depth factor δ (over a range of $0 < \delta \leq 0.25$) may be expressed as

$$\delta = \frac{K}{r \cdot \sqrt{\rho/\mu \cdot f}}$$

where

- K = 3168, a conversion constant,
- ρ volume resistivity (Ω-in) ($= 0.68 \cdot 10^{-6}$ for copper),
- f frequency (Hz).

For a low-frequency approximation of the response of the cable to a 5/50-ns pulse, the skin effect term can be neglected.

There are two types of capacitance associated with the cable (Fig. 16). The first is associated with the conductor-to-conductor capacitance, C_p. The other type of capacitance consists of equal valued capacitors C_{g1} and C_{g2}, which represent the two conductor-to-ground capacitances. The equation of the capacitance between two parallel cylinders representing the conductor-to-conductor capacitance may be written as [8]

$$C_p = \epsilon_r \cdot \frac{8.467 \cdot 10^{-3}}{\cosh^{-1}(d/2r)}$$

where C_p is the capacitance per unit length (μF/1000 ft) and ϵ_r is the relative dielectric constant of the material filling the space between the two conductors. The equation for the capacitance between a wire and a ground plane is similar; this capacitance is

$$C_g = \epsilon_r \cdot \frac{7.354 \cdot 10^{-3}}{\log_{10}(2H/r)}$$

where C_g is the capacitance per unit length (μF/1000 ft) and H is the distance between the conductor and the ground plane.

The resistance of the conductor is represented by resistance R_s in series with each inductance L_s. A resistance, R_p is in series with the capacitance C_p to simulate the losses encountered in the dielectric surrounding the two conductors. One additional resistance R_g simulates the resistance associated with the conductor-to-conductor leakage to complete the model.

Using the equations given, the following values were computed for a 1-m length of number 14/3 Type SO cable:

- L_s 261 nH, the series inductance of each conductor where $d = 0.45$ cm (0.177 in) and $r = 0.016$ cm (0.032 in);
- C_p 53 pF, the conductor-to-conductor capacitance assumes $\epsilon_r = 3$ for neoprene dielectric;
- C_g 17 pF, the conductor-to-ground capacitance;
- R_s 0.003 Ω, the series resistance of conductor (obtained from wire tables);
- R_p 10 Ω, the estimated resistance in series with C_p;
- R_g 10 MΩ, the estimated leakage resistance.

The velocity of propagation predicted by the model is approximately 170 m/μs for the 5/50-ns pulse traversing the neoprene-jacketed cable. In contrast, the higher velocities of propagation would be expected in the line enclosed by the steel conduit where the conductors have only a thin insulation surrounded by air. Measurements of the velocity of propagation confirm the difference between the two lines: 210 m/μs for the air-surrounded conductors in the conduit and 155 m/μs for the neoprene covered conductors.

REFERENCES

[1] *Electrical Fast Transient Requirements*. IEC Publication 801-4, Geneva, Switzerland, 1988.

[2] R. B. Bush, "Statistical considerations of electrostatic discharge evaluations," in *Proc. Int. Zurich Symp. Electromagnetic Compatibility*, 1987.

[3] F. D. Martzloff and P. F. Wilson, "Fast transient tests: Trivial or terminal pursuit?" in *Proc. Int. Zurich Symp. Electromagnetic Compatibility*, 1987.

[4] F. D. Martzloff, "The propagation and attenuation of surge voltages and surge currents in low-voltage ac power circuits," *IEEE Trans. Power App. Syst.*, vol. PAS-102, no. 5, May 1983.

[5] *Standard Surge Withstand Capability (SWC) Tests for Protective Relays and Relay Systems*, ANSI/IEEE C37.90.1, 1989.

[6] F. D. Martzloff and H. A. Gauper, "Surge and high-frequency propagation in industrial power lines," *IEEE Trans. Ind. Appl.*, vol. IA-22, no. 4, July/Aug. 1986.

[7] P. M. Rostek, "Avoid wiring-inductance problems," *Electron. Design*, Dec. 6, 1974.

[8] H. Pender and W. A. Del Mar, *Electrical Engineers' Handbook*. New York: Wiley (Engineering Handbook Series), 1949, p. 14–33.

François D. Martzloff (M'56–SM'80–F'83) completed his undergraduate studies in France and received the M.S.E.E. degree from the Georgia Institute of Technology, Atlanta, and the M.S.I.A. degree from Union College, Schenectady, NY.

After a long career at General Electric, he joined the staff of the National Bureau of Standards (now renamed National Institute of Standards and Technology) to work on conducted electromagnetic interference issues. His early experience covered high-voltage fuses, high-voltage bushings, and electronic power conversion; the latter marked a turning point to issues of overvoltage effects on semiconductors, surge suppression, metal oxide varistor applications, and interference mitigation. In addition to his research work on surge propagation and mitigation, he is contributing to the development of standards on surge environment and surge suppression within IEEE, ANSI, and IEC by documenting his measurements, as in the present paper, by presenting tutorials, and by drafting new standards.

Thomas F. Leedy (S'64–M'65) received the B.S. degree in physics from the American University, Washington, DC, and the M.S. degree in electrical engineering and the E.Ad. degree in engineering administration from George Washington University, Washington, DC, in 1965, 1972, and 1984, respectively.

From 1965 to 1980 he did research in microelectronics at the National Bureau of Standards where he developed and validated measurement methods for determining the effects of transient high-energy radiation on integrated circuits and for evaluating materials and processes of microelectronic device fabrication. Since 1980, he has been a member of the technical staff of the Electronic Instrumentation and Metrology Group of the Electrosystems Division where he has participated in the research program directed toward assuring the accuracy of automatic test equipment.

Mr. Leedy has served on numerous standards committees in microelectronics, computers, radiation effects, and electronic instrumentation for IEEE, ASTM, and the U.S. Department of Commerce International Trade Administration.